Contents lists available at SciOpen

Food Science and Human Wellness

journal homepage: https://www.sciopen.com/journal/2097-0765

China Food Publishing Co.

Fructooligosaccharides binding property of the LPxTG-motif surface protein derived from *Limosilactobacillus reuteri*

Jiang Liu[a,1], Mingjuan Ou[a,1], Ao Zhang[a], Yiping Yang[a], Xiaolu Li[a], Xiang Lu[a], Yuxing Guo[b], Daodong Pan[a], Tao Zhang[a,*], Zhen Wu[a,*]

[a] *College of Food Science and Engineering, Ningbo University, Ningbo 315211, China*
[b] *School of Food Science & Pharmaceutical Engineering, Nanjing Normal University, Nanjing 210097, China*

ARTICLE INFO

Article history:
Received 5 March 2024
Received in revised form 24 May 2024
Accepted 20 September 2024

Keywords:
Lactobacillus
LPxTG-motif surface protein
Fructooligosaccharides
Molecular docking
Molecular dynamics simulation
Adhesion property

ABSTRACT

As one of the adhesion-related surface factors on the cell wall of *Lactobacillus* strains, Leu-Pro-x-Thr-Gly (LPxTG) motif anchored proteins play a critical role in adhesion and molecular cross-talk with the host in the gastrointestinal tract (GIT). This study allows to understand that the combination of LPxTG-motif surface proteins (LMP) and fructooligosaccharides (FOS) can have a better promoting effect on lactic acid bacteria. In this study, molecular docking and molecular dynamics simulations were employed to investigate the interaction properties of LMP from *Limosilactobacillus reuteri* SH23 with small nutrient molecules in the host GIT. The thermodynamic parameters ΔG^0, ΔH^0, and ΔS^0 were calculated as −4.850 kJ/mol, −219.071 kJ/mol, and −718.501 J/(mol·K), respectively, for a binding constant of 1.414×10^4 μmol/L at 298.15 K. Fluorescence spectroscopy and circular dichroism spectroscopy were also utilised to study the interaction of LMP with the small nutrient molecules. It was found that LMP interacts with the small nutrient molecule FOS primarily through van der Waals and electrostatic forces. The transition from *β*-folding and random coiling to *α*-helix and *β*-sheet also indicates structural changes in the protein during the binding process. Furthermore, the binding of LMP to FOS not only improved the adhesion of the strain to intestinal epithelial cells and increased the auto-aggregation of the strain, but also promoted the growth of *L. reuteri* SH23. These findings provide a better understanding of *Lactobacillus* and host interactions at the cell surface protein level.

1. Introduction

The gastrointestinal tract (GIT) is probably one of the complex systems in the human body, occupied not only by trillions of microorganisms (bacteria, archaea, fungi, probiotics, and viruses) and is full of proteases, acidic pH and high bile salts necessary for food digestion[1]. Meanwhile, internal acidification also decreases the activity of acid-sensing enzymes and the survival of bacteria in this irritant urethra[2]. Lactic acid bacteria (LAB) are the predominant microorganisms in food and they play an important role in the health of the human GIT[3]. Also, GIT health promotion has received considerable attention in the last decade[4]. It was found that the adhesive properties of bacteria are one of the key prerequisites for mucosal surfaces to resist transient colonization by inactive organisms from the GIT, and that their surface proteins are one of the important components of adhesive properties[5-7].

Most surface proteins are classified into 4 major groups: i) transmembrane proteins, ii) lipoproteins, iii) Leu-Pro-x-Thr-Gly (LPxTG)-like proteins, and iv) cell wall binding proteins, also a subset of proteins that are exposed to the bacterial cell surface and therefore interact with the extracellular environment constitute the surface[8-9]. LPxTG-motif surface proteins (LMP) are a family of proteins characterized by an LPxTG-like sequence located at the

[1] These authors contributed equally to this work.
[*] Corresponding authors at: College of Food Science and Engineering, Ningbo University, Ningbo 315211, China.
Email address: zhangtao@nbu.edu.cn (T. Zhang); woodsen@163.com (Z. Wu)
Peer review under responsibility of Beijing Academy of Food Sciences.

SciOpen Publishing services by Tsinghua University Press

http://doi.org/10.26599/FSHW.2024.9250388

C-terminus of the protein, which sequence is recognized and cleaved by a trans enzyme called proenzyme, which is covalently anchored to the surface protein on the cell wall peptidoglycan[10]. LAB surface proteins containing LPxTG motifs have been reported to enhance not only intestinal adhesion but also resistance to gastrointestinal digestive enzymes during gastrointestinal colonisation[11]. It was shown that *Lactobacillus rhamnosus* GG MBF, an active mucus-specific surface adhesion protein, may be involved in hair follicle-mediated mucus adhesion and is important in bacterial adhesion to the intestine[12]. Fructooligosaccharides (FOS) are abundant in nature and are commonly used as prebiotics. They can be combined with probiotics to effectively reduce intestinal inflammation and regulate gut flora. *In vivo* studies have demonstrated that FOS as prebiotics enhance the growth of lactobacilli both inside and outside the intestines and extend the colonisation time of *Lactobacillus* in the intestines, thereby improving the intestinal micro-ecological environment[13]. Our previous result also found that LMP can improve the survival of lactic acid bacteria in the harsh GIT environment, but whether the interaction between LMP and small molecules can better improve the functional role of lactic acid bacteria in the survival of the GIT needs to be elucidated in further studies.

The recent surge in bioinformatics based on the analysis of genomic data, together with the development of several available new genetic tools, also motivates further studies aimed at uncovering adhesion factors of LAB by using sequence information stored in surface proteins[14]. Molecular modeling docking is one of the most widely used virtual screening methods, and the purpose of molecular docking is to predict the image of small molecule ligands binding to a suitable target site. Molecular simulation of docking allows rapid assessment of the conformation of proteins, predicts their binding to other molecules, and simulates intermolecular interactions[15-17]. When proteins are involved in various processes, such as ligand binding, it may change their structure. Also, the binding sites and parameters related to the kinetic and conformational changes caused by ligand binding need to be identified[18-19]. Molecular dynamics (MD) simulation is a computational technique used to model the movement of proteins, molecules, and atoms within a molecular system, as well as their interactions. These simulations can replicate the dynamic behavior of molecular systems under varying temperatures, pressures, and other external conditions. This includes processes like protein folding, ligand binding, and protein interactions[20-21]. Presently, molecular dynamics simulations are extensively employed in diverse fields such as medicine and biology, often in conjunction with various biological techniques like X-ray diffraction (XRD), multi-spectroscopic, and Zeta potential[22-24]. Fluorescence spectroscopy (FL) and circular dichroism (CD) reflect the interactions between proteins and small molecules, the interaction forces between molecules, and the changes in protein structure through fluorescence changes[25-28].

Nowadays, there are many methods to explore the interaction between small molecules, and this paper focuses on bioinformatics, molecular modeling docking, FL, CD, cell adhesion and growth status to demonstrate the interaction between small molecules and proteins. The aim of this study was to investigate the interactions between LMP and various small molecule nutrients using molecular docking simulation methods. In addition, the reliability of the binding affinity results from molecular docking simulations was verified by CD and FL. In addition, the interaction of LMP with small molecule nutrients on the adhesion properties of *Lactobacillus* and the growth characteristics were both investigated. The findings of these results will lead to a better understanding of the host interactions of LAB in the GIT environment.

2. Materials and methods

2.1 Strains and culture

L. reuteri SH23 was obtained from the China General Microbiological Culture Collection Center (Beijing, China). Bacteria are cultured in de Man-Rogosa-Sharpe (MRS) media at 37 ℃ for 16 h before use. FOS were purchased from Yuanye Biotech (Shanghai, China) and diluted with ultrapure water. Caco-2 cells purchased from Boster Biotechnology (Wuhan, China) were cultured in Dulbecco's modified Eagle's medium (Sigma-Aldrich, Darmstadt, Germany) supplemented with 10% heat-inactivated fetal bovine serum (FBS), 1% nonessential amino acids, 100 U/mL penicillin and 100 mg/mL streptomycin. The cells were cultured at 37 ℃ in a humidified atmosphere of 5% CO_2.

2.2 LMP preparation

Based on the former results, the expression of LMP (A4V07_06340, UniProt) was screened from transcriptomic and proteomic data and was upregulated in both stimulated gastric and intestinal fluids[29]. A4V07_06340 (A0A1X8VAD2) was selected in proteomics associated with LPxTG patterns. Total DNA was isolated from bacteria using the method described in the easy Pure Rapid Gel Extraction Kit (Transgenic, Pecking, China). PCR amplification primers were used as follows: F (5′-AATTCGCTGACTTAACAA TCGTGGATCAA-3′); R (3′-CTCGAGCTAATCTTCTTTGCGCC GTTTC-5′). The sequence of the protein gene was ligated into the expression vector pET-32a and overexpressed in BL21 (DE3) cells. The target protein was induced with 0.4 mmol/L isopropyl-*β*-*D*-thiogalactoside (IPTG), then disrupted by sonication (working for 3 at 10 s intervals, working 80 times), centrifuged, and the supernatant was removed and eluted with 80 mmol/L elution buffer (80 mmol/L imidazole, 20 mmol/L Tris, 0.5 mmol/L NaCl, pH 8.0). After that, the peak solution was collected and verified by SDS-PAGE (12% polyacrylamide), and the protein concentration was determined using the BCA method (Sangon Biotech Co., Ltd., Shanghai, China). The purified proteins were collected and freeze-dried for further use.

2.3 Molecular docking simulation

The online database PDB (PDB id: 4mt5) files of relevant multifunctional proteins were screened through the NCBI website and SWISS-MODEL (https://swissmodel.expasy.org) for further use; the ligands were selected as shown in Table 1, mainly polysaccharides, fatty acids and some common small molecules such as metal ions, and The PDB structure files of the ligands were downloaded through the pub Chem website, and the Babel 2.3.2 software was opened to convert the ligand files into PDB files, which can be used for docking calculations of the relevant molecules through the Autodock Vina 1.1.2 (Scripps Research Institute, USA) software[30]. As shown in Table 1, the interactions between proteins and common intestinal

small molecules, mainly polysaccharides, fatty acids, and some common small molecules such as metal ions, result in binding.

2.4 MD simulation

Protein-ligand (LMP and FOS) complexes obtained *via* molecular docking were subjected to molecular dynamics simulations using GROMACS. The AMBER force field was applied for the protein, and GAFF for the ligand, while the TIP3P water model was used to solvate the system, forming a water box with a periodic boundary of 1.2 nm. Sodium and chloride ions were added to neutralise the system, closely mimicking experimental conditions. Before the main simulations, the complexes underwent 3 000 steps of energy minimisation in a vacuum using the steepest descent method to eliminate atomic overlaps. After solvation with TIP3P water, the system was further energy-minimised under position restraints, followed by solvent relaxation under NVT and NPT ensembles. The position restraints were then removed, and the entire system was simulated for 50 ns under NPT conditions. During the MD simulations, all C−H and O−H bond lengths were constrained using the LINCS algorithm, with a time step of 2.0 fs. The temperature was maintained at 298.15 K using a V-rescale thermostat with a coupling time of 1.0 ps, while pressure was controlled at 1 bar using a Parrinello-Rahman barostat with a coupling time of 2.0 ps. The simulations were carried out over 50 000 ps at ambient temperature and pressure. From the MD simulations, variations in hydrogen bonding between LMP and FOS, as well as root mean square deviation (RMSD), root mean square fluctuation (RMSF), and radius of gyration (Rg), were analysed.

2.5 FL and CD analysis

The binding properties of LMP to the screened FOS were determined by a slightly modified fluorescence spectroscopy assay by Guimarães et al.[38]. Measurement conditions were as follows: the excitation wavelength was 280 nm and the emission wavelength range is 308−450 nm. LMP protein solution (0.8 mg/mL) and different concentrations of FOS (26.67, 31, 36, 40 mmol/L) were added into the centrifuge tube. After the reaction at room temperature for 5 min, 200 μL of the prepared sample solution was absorbed into the 96-well plate, and the experimental determination was carried out by fluorescence photometer (Hitachi F-4700, Japan). The interaction mechanism between proteins and small molecules was also analyzed by CD spectroscopy, which scans from 190 to 260 nm[39].

2.6 Microscale thermophoresis (MST) analysis

The fluorescent dye used in this experiment was RED-Tris-NTA protein labeling kit and capillaries were purchased from Nano Temper. The excitation and emission wavelengths were 605−645 and 680−685 nm, respectively, and the temperature for MST was set at 37 °C. The LMP protein concentration was 200 nmol/L, and the small molecule concentrations were 25, 40, and 80 μmol/L, respectively. the LMP was labeled with fluorescent dye, and then mixed with the small molecule series dilutions, filled capillary tubes into the loading tray, and then the results were analyzed and calculated by the software.

2.7 Adhesion-assistant properties of LMP

First, the effect of the tested molecules on cell viability was verified by first measuring the cell viability in the tested solution with the Cell Counting Kit-8 (CCK-8)[40] to verify the effect of the test molecules on cell viability in the groups of control, single protein, single small molecule, low concentration mixture (FOS 26.67 mmol/L) and high concentration mixture (FOS 40 mmol/L). Then, 10 μmol/L fluorescein isothiocyanate (FITC) was added to *L. reuteri* SH23 (1×10^8 CFU/mL), and the mixture was incubated in the dark for 30 min (37 °C). The fluorescence intensity of labeled *L. reuteri* SH23 (excitation wavelength, 485 nm; emission wavelength, 538 nm) was measured as the initial fluorescence value (A_0). The labeled bacterial suspension and different concentrations of recombinant expression proteins were added to 96 wells and incubated with Caco-2 cells for 2 h. The final fluorescence intensity was measured after washing twice with PBS as the post-elution fluorescence value (A_1). The calculation formula of the adhesion rate of *L. reuteri* SH23 is as follows:

$$\text{Adhesion rate of bacteria (\%)} = \frac{A_1}{A_0} \times 100 \quad (1)$$

2.8 Auto-aggregation of the strain

L. reuteri SH23 was cultured to the logarithmic growth phase. The cells were then washed 3 times with PBS and resuspended in PBS to achieve an $OD_{600\ nm}$ of 1.00 ± 0.05. Subsequently, *L. reuteri* SH23 was inoculated into fresh MRS broth containing 5 mg of LMP and 10 mg of FOS, respectively, and cultured for 6 h. The culture was centrifuged at 6 000 r/min for 5 min at 4 °C, and the $OD_{600\ nm}$ of the bacterial suspension was adjusted to 1.00 ± 0.05 (A_0) by washing three times with PBS. To assess the auto-aggregation of bacterial cells, 4 mL of the suspension was transferred into a 10 mL centrifuge

Table 1
Common prebiotics in the GIT.

Substance	Function	Year	Reference
Galactooligosaccharides (GOS)	GOS modulated homeostasis of the aging gut by promoting changes in the microbiome composition and host gene expression	2021	[31]
Bifidobacterium infantis and xylooligosaccharide (XOS)	Alleviates dextran sulfate sodium-induced ulcerative colitis	2020	[32]
Fructo-, galacto-, and mannan-oligosaccharide	Protect against 5-fluorouracil-induced intestinal mucositis in rats	2019	[33]
Butyrate	Attenuates gastrointestinal salmonella disease	2018	[34]
Docosahexaenoic acid (DHA) and eicosapentaenoic acid (EPA)	Improve the abnormal contractile functions of the LGI tract associated with inflammatory diseases	2021	[35]
Flaxseed fiber (FF) and/or dairy calcium (Ca)	Binding liquid fats to more solid complexes	2017	[36]
Zinc (Zn)	Understand the pathogenesis and progression of liver and gastrointestinal disease	2008	[37]

tube and left to stand at room temperature for 12 h. The suspension was then used to measure the $OD_{600\ nm}$ (A_1). The auto-aggregation was calculated by using the following equation:

$$\text{Auto-aggregation}\ (\%) = (1 - \frac{A_1}{A_0}) \times 100 \quad (2)$$

2.9 Growth curve measurement

L. reuteri SH23 were activated in MRS broth 2−3 times. The bacterial solution was washed 3 times with PBS and adjusted $OD_{600\ nm} = 1$. The final concentrations of LMP and FOS in MRS medium were 0.3 and 0.5 mmol/L. *L. reuteri* SH23 inoculated into 50 mL of an MRS medium at an inoculum volume of 1:100, and incubated at 37 °C for 24 h. Subsequently, the $OD_{600\ nm}$ value was measured every 2 h and the absorbance was calibrated using blank MRS as the control; the growth curve was generated with the measured OD value as the ordinate.

2.10 Statistics analysis

All experiments were performed in triplicate and the results were expressed as means ± standard deviation (SD). Significance levels were analyzed by ANOVA test ($P < 0.05$) using SPSS Statistics 26 (SPSS Inc, IBM, New York, USA), and GraphPad Prism 8, Origin 2018 software was used for graphing.

3. Results

3.1 LMP identification

The target gene (Fig. 1A, 3 042 bp) was overexpressed in the recombinant expression plasmid pET-32a-A4V07_06340 (Fig. 1B), and after transfer into BL21 (DE3) cells, the bacteria were induced to produce LMP with 0.4 mmol/L IPTG (25 °C, 6 h). Based on the overexpression result, the molecular weight of the purified LMP was approximately 140 kDa (Fig. 1A).

3.2 Molecular simulation docking results

As shown in Table 2, the binding energy of LMP to FOS was −5.5 kcal/mol, the lowest value among all the molecular docking binding simulations, indicating a strong binding interaction between LMP and FOS. As shown in Fig. 2, a diagram of the interactions between LMP and small molecules is presented using molecular modeling docking technique, and the optimal sites of interaction between small molecules different from each other will also produce corresponding changes. In addition, the binding mode between receptor proteins LMP and FOS was investigated by molecular docking. The binding pattern exhibited by amino acid residues between receptor protein 4mt5 and FOS ligand small molecules is shown in Fig. 2A, where LMP and FOS can form hydrogen bonds with V46, E41, H71, N120, M73, T74, T118, T76, D77, Y116, D80, and N82. It is hydrophobic with L47, K7, Y45, G44, G72, N120, and H75.

Table 2
Molecular simulation docking screening of the affinity between the LMP protein and different small molecule nutrients.

Protein	Substance	Affinity (kcal/mol)
4mt5_protein	FOS	−5.5
4mt5_protein	Phenyllactic acid	−5.1
4mt5_protein	DHA	−4.7
4mt5_protein	EPA	−4.5
4mt5_protein	*D*-Glucitol-1,6-bisphosphate	−4.1
4mt5_protein	Arachidonic acid	−4.1
4mt5_protein	*L*-Lactic acid	−3.7
4mt5_protein	*D*-Lactic acid	−3.6
4mt5_protein	Butyric acid	−3.1
4mt5_protein	Calcium	−1.2
4mt5_protein	Fe	−1.2
4mt5_protein	Mg	−1.2
4mt5_protein	Zn	−1.2

Note: 4mt5_protein is in the database with A4V07_ 06340 with the highest protein match.

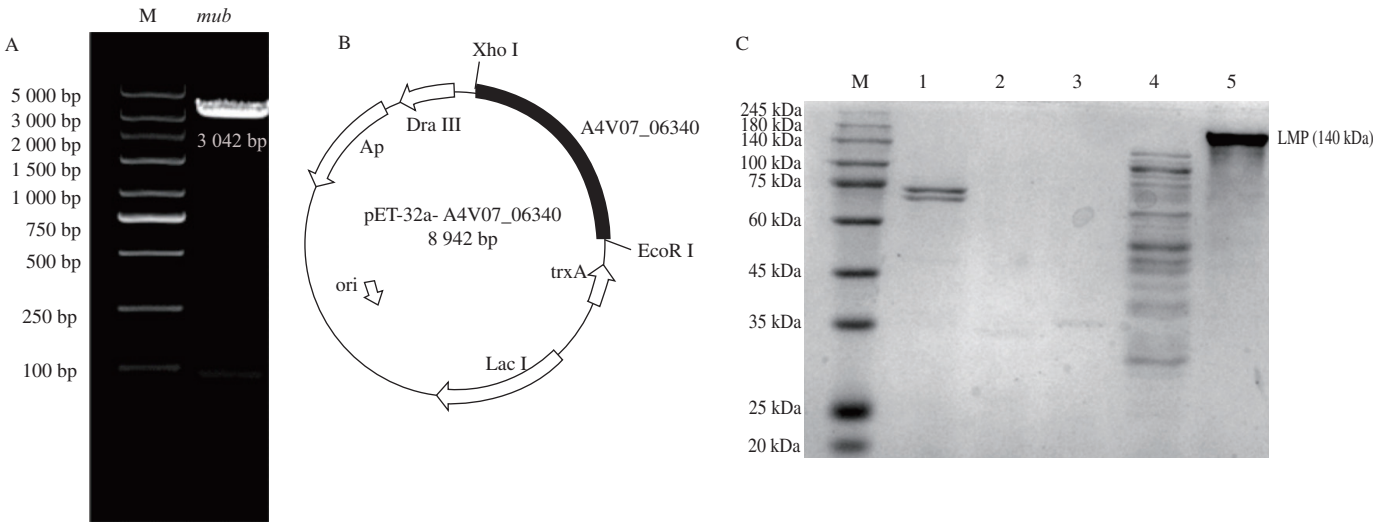

Fig. 1 Overproduction and purification of LMP derived from the *L. reuteri*. (A) PCR amplification product of the target LMP gene; (B) recombinant expression plasmid construction map; (C) identification of the recombinant LMP with SDS-PAGE, lane 1 is crude whole-cell protein extracts after induction, lanes 2–4 is the uninduced bacteriophage protein, and line 5 is the purified LMP protein.

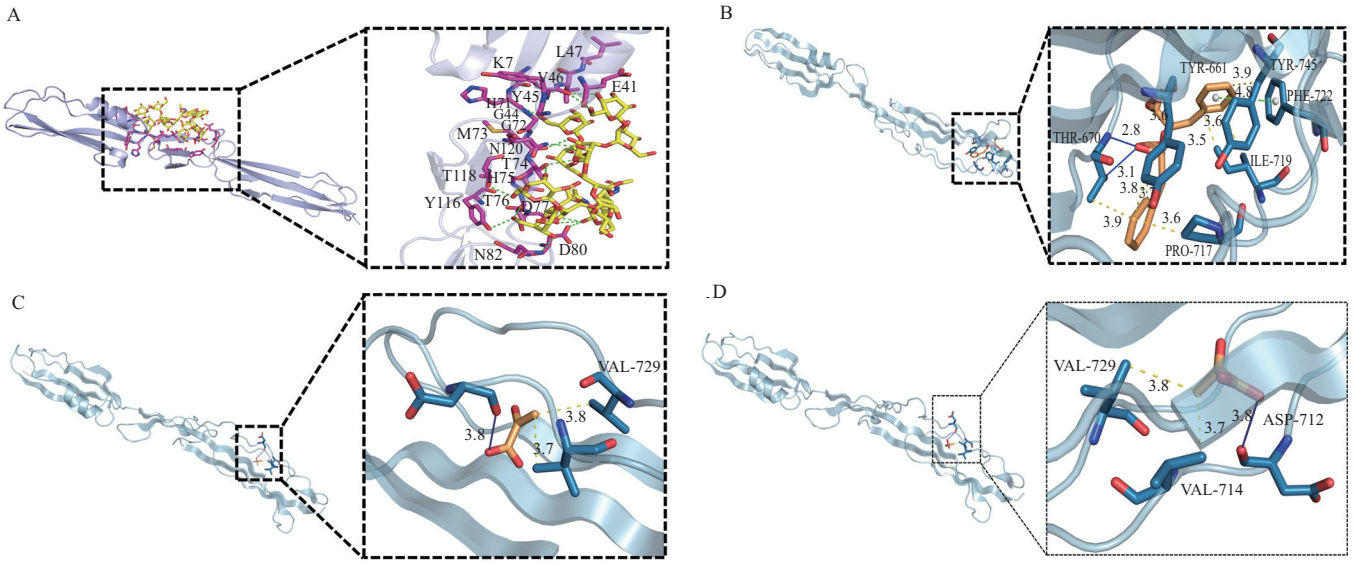

Fig. 2 Molecular simulation of LMP interactions with small molecules docking the interaction between LMP and FOS (A); interaction of phenyl lactate with LMP (B); molecular docking simulation between *L*-lactic acid and LMP (C); molecular docking simulation between *D*-lactic acid and LMP (D).

3.3 Analysis of MD simulation results

Through molecular dynamics simulations, the interaction between LMP and FOS was found to have a binding constant of 1.414×10^4 μmol/L, as well as thermodynamic parameters ΔG^0, ΔH^0, and ΔS^0 at 298.15 K. These values are −4.850 kJ/mol, −219.071 kJ/mol, and −718.501 J/(mol·K), respectively, indicating that the binding process is exothermic. The negative ΔG^0 value suggests that the interaction is spontaneous. In this study, the interactions between LMP and FOS were primarily driven by electrostatic and van der Waals forces. MD simulations were used to further explore the conformational changes and structural stability of the LMP and FOS complexes, validating and complementing the molecular docking results. As shown in Fig. 3A, the RMSD trajectories of LMP and LMP-FOS complexes were similar, with fluctuations within 0.5 nm, indicating no significant structural changes during the simulation. The flexibility and local mobility of each residue in the LMP-FOS complex were investigated using RMSF trajectories. Residues 1204–1216, 1220–1231, 1250–1267, and 1286–1300 showed higher fluctuations, likely due to their involvement in protein-protein interactions (Fig. 3B). The Rg indicated that the LMP and FOS complexes remained structurally stable throughout the simulation, with minimal fluctuations (Fig. 3C). To investigate the hydrogen bonding properties of the binding sites, the number of key hydrogen bonds stabilizing the LMP-FOS complexes was calculated. As shown in Fig. 3D, the number of hydrogen bonds remained stable at 5 or more throughout the simulation, indicating strong hydrophobic interactions and the formation of highly stable complexes.

3.4 Fluorescence spectrum and CD measurements

Corrections have been made to account for the inner filter effects in the fluorescence measurements. As shown in Fig. 4A, the fluorescence intensity of LMP solution decreased with the increase of FOS concentration, which may be due to the quenching effect of FOS on LMP, indicating the interaction between amino acid residues of LMP and FOS. In general, the absorption wavelength peak of LMP was around 325 nm, and as the ratio of FOS/LMP increased from 1:6 to 1:9 the fluorescence intensity value at this point tended to decrease, i.e., the concentration of LMP protein solution was (0.8 mg/mL) and FOS concentration was 26.67, 31, 36, 40 mmol/L (Fig. 4A). Meanwhile, a blue shift (198−190 nm) was found in the CD spectrum of the mixture of LMP (lowest CD signal 220 nm, Fig. 4B) and FOS, and the negative peak appeared red-shifted with the change of LMP concentration in the LMP+FOS solution (Fig. 4C). As shown in Table 3, at a ratio of LMP to FOS of 1:8, the *α*-helix content increased significantly to 57.4%, while the *β*-sheet content decreased. This change is likely due to the addition of FOS, which provides stability or forms new hydrogen bonds and hydrophobic interactions, promoting the formation of *α*-helices and converting regions that might otherwise form *β*-sheets into *α*-helices. MD simulations indicate that the interaction between LMP and FOS is primarily governed by van der Waals forces and electrostatic forces. Van der Waals forces influence protein folding and the formation of secondary structures between FOS and LMP. FOS contains charged groups that interact with the charged amino acid side chains in LMP, thereby enhancing the stability of specific secondary structures. Overall, the random coil content decreased, suggesting that the addition of FOS induces LMP to form more ordered secondary structures and reduces the disordered random coils. Furthermore, as shown in Fig. S1, the data points were fitted to obtain the binding parameters (binding affinity). It is clear that the binding capacity between LMP and FOS under conditions such as the acceptable range of homogeneity is in the range of 2−8 μmol/L.

3.5 Liability and adhesion enhancement of LMP coupled with FOS on L. reuteri SH23

As shown in Fig. 5A, the results with CCK-8 reagent showed that their cell viability were higher than 100%, indicating that the protein as well as the small molecules were not toxic to the cells. Meanwhile, according to the results of adhesion analysis, the addition of recombinant protein could improve the adhesion

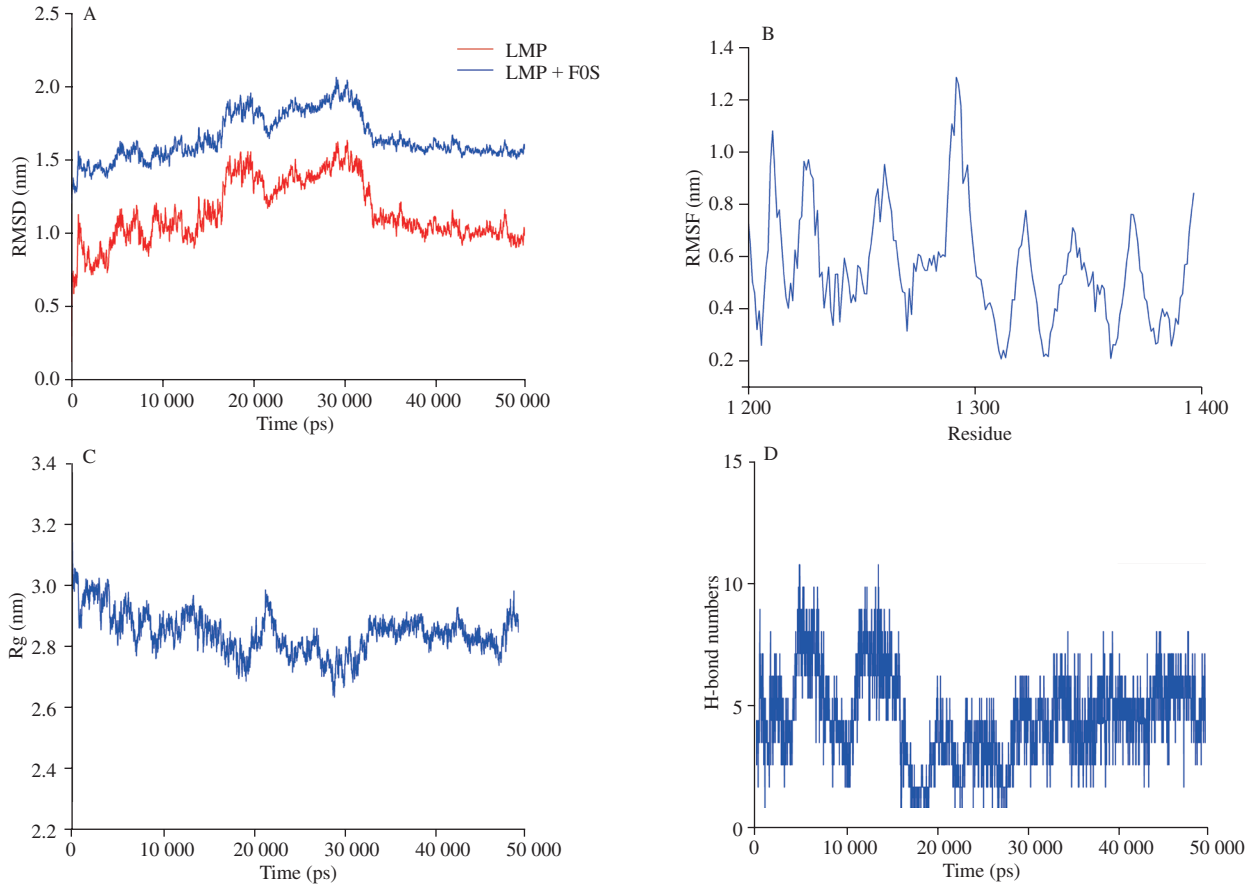

Fig. 3 Results of molecular dynamics. (A) RMSD; (B) RMSF; (C) Rg; (D) The number of hydrogen bond.

Table 3
Secondary structural changes (%) of the LMP interact with different concentrations of FOS.

Sample proportion	*α*-Helix	*β*-Sheet	*β*-Turn	Random coil
LMP	21.77	36.37	16.33	25.67
1:6	27.4	54.3	0	18.3
1:7	29.1	52.9	0	17.9
1:8	57.4	22.9	0	19.6
1:9	40.9	41.2	0	17.9

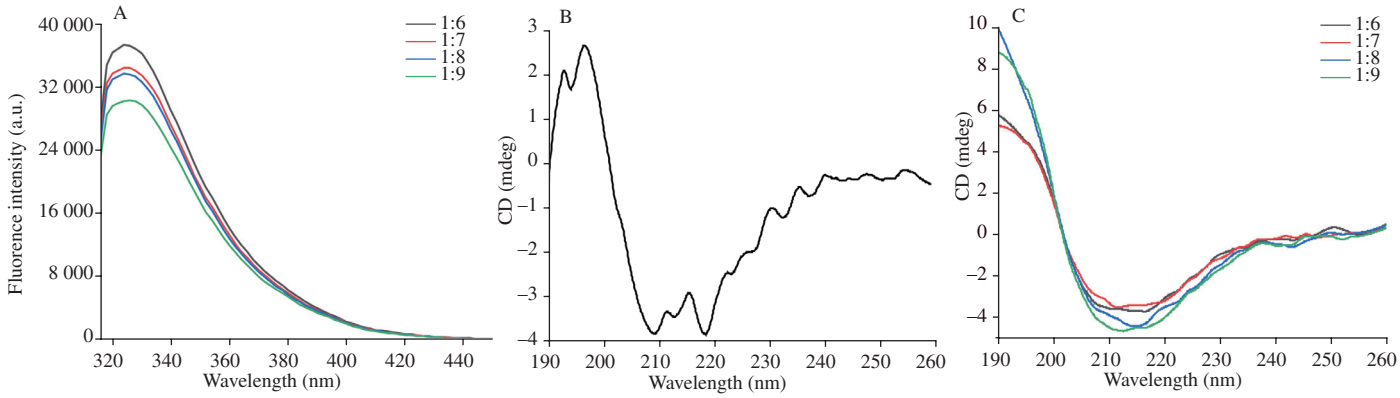

Fig. 4 Spectral properties of LMP-FOS interactions; the simulated docking illustration of LMP with FOS; (A) the fluorescence intensity spectra of LMP and FOS mixture (ratio 1:6−1:9) at 25 °C; (B) CD analysis of the single LMP; (C) CD analysis of the LMP with FOS mixture (ratio 1:6−1:9).

rate of *L. reuteri* SH23 to Caco-2 cells, as shown in Fig. 5B, when 80 μg/mL recombinant protein was added, the adhesion rate was as high as 7.11%. When FOS was added in the *in vitro* normal model, divided into low concentration group (FOS 26.67 mmol/L) and high concentration group (FOS 40 mmol/L), the adhesion rate was much higher than the other 2 groups (no LMP and no FOS), and the adhesion power of FOS high concentration group was as high as 7.65%. As shown in Fig. 5C, the cell adhesion in the 5 groups, the trend was consistent with that in Fig. 5B above. Fig. 5C (a and c) shown the cell adhesion effect was significantly different from that of Fig. 5C (b, d and e). It indicates that LMP and LMP+FOS can promote the adhesion between cells and *L. reuteri* SH23, which can further reduce the contact area between *L. reuteri* SH23 and gastrointestinal fluid, slowing down the damage caused by direct contact and having a protective effect.

3.6 Auto-aggregation and growth status of the strains results analysis

As shown in Fig. 6A, the average auto-aggregation of the control, LMP, FOS, and LMP-FOS complexes were 17.10%, 21.57%, 20.98%, and 30.56%, respectively. The results indicate that both LMP and FOS promote the auto-aggregation of *L. reuteri* SH23. However, the LMP-FOS complex significantly enhances auto-aggregation more than either LMP or FOS alone. As shown in Fig. 6B, at 6 h *L. reuteri* SH23 entered the logarithmic growth phase, but compared to control, LMP and FOS, *L. reuteri* SH23 grew the fastest after the addition of LMP+FOS (Table 4). It indicates that the interaction of LMP and FOS can better promote the growth of *L. reuteri* SH23.

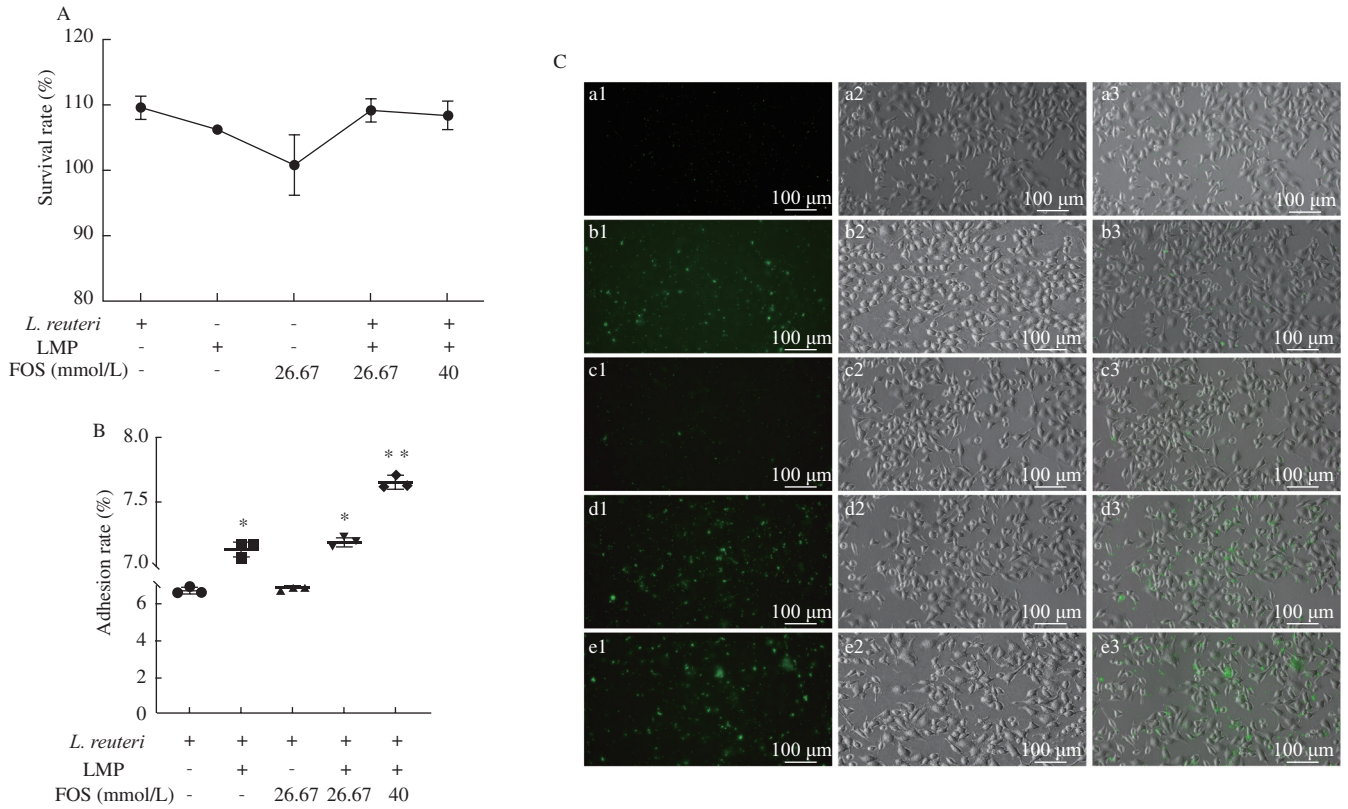

Fig. 5 Toxicological properties of LMP, FOS and *L. reuteri* SH23 on Caco-2 cells. Toxicological validation of FOS (A); adhesion of LMP and FOS to *Lactobacillus* under normal conditions (B); actual fluorescence plots of cell adhesion for each group (C). Letters represent groups, a, *L. reuteri* SH23; b, *L. reuteri* SH23+LMP; c, *L. reuteri* SH23+FOS; d, *L. reuteri* SH23+LMP+*D*-FOS; e, *L. reuteri* SH23+LMP+H-FOS; numbers represent scenes; 1, fluorescence image; 2, bright field image; 3, confocal image. $^{**}P < 0.01$, $^{*}P < 0.05$.

4. Discussion

Among the microorganisms in the complex ecosystem of the human GIT, LAB are Gram-positive bacteria that are probiotics that contribute to host health. As commonly used strains, *Lactobacillus* can inhabit this harsh GIT, which is essential for gut-microbe homeostasis[41-43]. Research has shown that gram-positive *Lactobacillus* have evolved a variety of different mechanisms of intestinal adaptation that ultimately play a health-promoting role in the host[44], and this mechanism of action may be related to proteins on the surface of the cell wall. It has been demonstrated that surface proteins such as mucus binding proteins can promote the aggregation and formation of membrane-like morphologies of *Lactobacillus* strains, leading to improved bacterial survival in the GIT[45-46].

Moonlighting proteins are proteins that serve roles at various sites[47]. Adhesion occurs through interactions between macromolecules on the bacterial cell wall and proteins or glycoproteins on the enterocyte surface, and one important approach is the anchoring of carboxyl termini by LMP on the bacterial surface[48-50]. Having established that LMP has adhesive properties

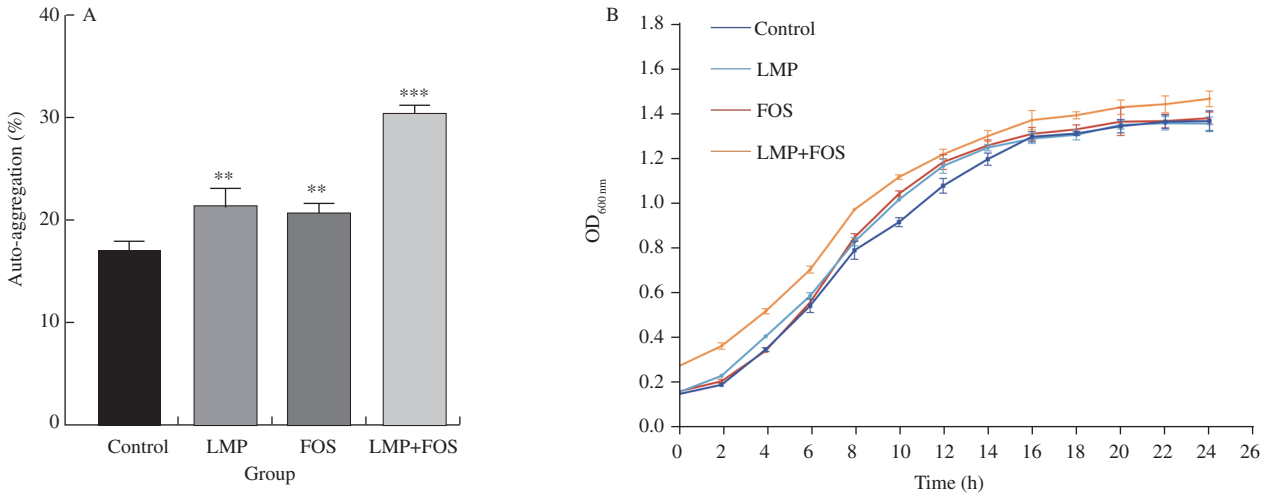

Fig. 6 Four different lines related to the control, single treatment of LMP and FOS, and the both LMP and FOS treated group. (A) The effect of LMP and FOS on the auto-aggregation capacity of *L. reuteri* SH23; (B) growth status of *L. reuteri* SH23 upon LMP and FOS. ***$P < 0.001$, **$P < 0.01$.

Table 4
Effect of the LMP and FOS on the growth status of *L. reuteri* SH23 in the different culture times.

Time (h)	Control	LMP	FOS	LMP+FOS
0	0.17 ± 0.01^{c}	0.18 ± 0.00^{b}	0.18 ± 0.00^{b}	0.30 ± 0.00^{a}
2	0.21 ± 0.02^{c}	0.26 ± 0.00^{c}	0.23 ± 0.01^{b}	0.40 ± 0.02^{a}
4	0.38 ± 0.01^{c}	0.44 ± 0.01^{c}	0.37 ± 0.00^{b}	0.56 ± 0.01^{a}
6	0.58 ± 0.03^{b}	0.63 ± 0.01^{b}	0.6 ± 0.01^{b}	0.75 ± 0.02^{a}
8	0.84 ± 0.04^{c}	0.88 ± 0.02^{bc}	0.91 ± 0.02^{b}	1.03 ± 0.01^{a}
10	0.98 ± 0.02^{c}	1.08 ± 0.01^{b}	1.11 ± 0.01^{b}	1.19 ± 0.01^{a}
12	1.14 ± 0.03^{b}	1.24 ± 0.03^{a}	1.26 ± 0.03^{a}	1.29 ± 0.02^{a}
14	1.27 ± 0.03^{b}	1.32 ± 0.02^{ab}	1.33 ± 0.03^{a}	1.38 ± 0.03^{a}
16	1.37 ± 0.02^{ab}	1.37 ± 0.02^{b}	1.39 ± 0.03^{ab}	1.45 ± 0.03^{a}
18	1.39 ± 0.01^{b}	1.38 ± 0.02^{b}	1.41 ± 0.02^{b}	1.48 ± 0.02^{a}
20	1.43 ± 0.03^{a}	1.43 ± 0.02^{a}	1.45 ± 0.06^{a}	1.51 ± 0.03^{a}
22	1.46 ± 0.03^{ab}	1.44 ± 0.03^{b}	1.45 ± 0.03^{ab}	1.53 ± 0.04^{a}
24	1.45 ± 0.05^{b}	1.44 ± 0.03^{b}	1.46 ± 0.03^{b}	1.55 ± 0.04^{a}

Note: Different lowercase letters in same row indicate significant difference ($P < 0.05$).

through previous studies of LAB surface proteins[51], the present study sought to explore another function of LMP interacting with small molecule nutrients to enhance adhesion properties and promote gastrointestinal tolerance[52-53].

Previous studies have shown that some surface proteins anchored to the peptidoglycan layer derived from yeast or *Escherichia coli* have metal-binding properties[54], and some researchers also found the cell wall-related proteins of the *Clostridioides difficile* have polysaccharide interaction functions[55]. By studying the interaction of LMP with small molecules, it was found that the binding affinity of metals to small-molecule nutrients is different from that of molecule-macromolecule interactions. MD simulations revealed that the interaction between LMP and FOS small molecules primarily relies on van der Waals and electrostatic forces.

Also, the weak fluorescence intensity of the LMP-FOS mixture with increasing FOS concentration confirmed the conformational changes in the protein structure, which may be due to the conversion of the α-helix structure to the β-sheet and β-turn structure due to partial unfolding of the protein[56]. Along with the change in the secondary structure of LMP, the adhesion of the protein was further verified in the adhesion model to the Caco-2 cell line[57-58]. In contrast, the removal of surface-bound proteins reduced the adhesion-associated surface proteins of *Lactobacillus plantarum* 423 and the adhesion between *L. plantarum* and Caco-2 cells by 40%[59-60]. The addition of recombinant proteins promoting bacterial aggregation can reduce the contact area of *L. reuteri* SH23 with gastrointestinal fluids, thereby mitigating damage from direct contact. LMP enhances this protective effect under normal conditions, while FOS further improves the adhesion of *L. reuteri* SH23 to intestinal epithelial cells and its auto-aggregation ability. This combination effectively enhances the gastrointestinal tolerance of LAB. Additionally, the inclusion of LMP and FOS complexes supports the growth of *L. reuteri* SH23.

5. Conclusions

In summary, the study demonstrated that the LPxTG-motif protein interacts with FOS through van der Waals and electrostatic forces, resulting in the transformation of β-sheet and random curling into α-helix and β-turn structures. Additionally, binding LMP to FOS significantly increased the adhesion rate of *L. reuteri* SH23 to Caco-2 cells, enhanced the strain's adhesion ability to intestinal epithelial cells, elevated its auto-aggregation, and improved its growth rate. These findings provide insights into the role of LMP as a multifunctional protein in the cell wall of *L. reuteri* SH23.

Conflict of interest statement

All authors involved in this article confirm that they have no conflict of interest in the work described in this manuscript. This article does not contain any studies with human participants or animals performed by any of the authors.

Acknowledgment

This work was supported by the Outstanding Youth Fund of Zhejiang Province (LR22C200001), the National Natural Science Foundation of China (32472356, 32072192, 32402125), the Key Project of Ningbo Science and Technology (2023Z127), the Key Research and Development Project of Zhejiang Province (2020C02042), the Open Project Program of the First-Class Bioengineering Disciplines in Zhejiang Province (KF2023004), the Student Research and Innovation Program of Ningbo University (2023SRIP3603, 2023SRIP3616), the K. C. Wong Magna Fund in Ningbo University.

Appendix A. Supplementary data

Supplementary data associated with this article can be found, in the online version, at http://doi.org/10.26599/FSHW.2024.9250388.

References

[1] C. Meng, C. Bai, T.D. Brown, et al., Human gut microbiota and gastrointestinal cancer, Genom. Proteom. Bioinform. 16 (2018) 33-49. https://doi.org/10.1016/j.gpb.2017.06.002.

[2] S. Lebeer, J. Vanderleyden, S.C.J. De Keersmaecker, Genes and molecules of lactobacilli supporting probiotic action, Microbiol. Mol. Biol. Rev. 72 (2008) 728-764. https://doi.org/10.1128/mmbr.00017-08.

[3] S. Beglari, S. Fereshteh, M. Milani, et al., Lactoremediation: heavy metals elimination from the gastrointestinal tract by lactic acid bacteria, Food Biosci. 56 (2023) 103202. https://doi.org/10.1016/j.fbio.2023.103202.

[4] F. Yan, D.B. Polk, Probiotics and probiotic-derived functional factors—mechanistic insights into applications for intestinal homeostasis, Front. Immunol. 11 (2020) 1428. https://doi.org/10.3389/fimmu.2020.01428.

[5] F.J. Carr, D. Chill, N. Maida, The lactic acid bacteria: a literature survey, Crit. Rev. Microbiol. 28 (2008) 281-370. https://doi.org/10.1080/1040-840291046759.

[6] J. Walter, Ecological role of lactobacilli in the gastrointestinal tract: implications for fundamental and biomedical research, Appl. Environ. Microbiol. 74 (2008) 4985-4996. https://doi.org/10.1128/aem.00753-08.

[7] S.S. Yoon, J. Sun, Probiotics, Nuclear receptor signaling, and anti-inflammatory pathways, Gastroenterol. Res. Pract. 2011 (2011) 1-16. https://doi.org/10.1155/2011/971938.

[8] M. Desvaux, E. Dumas, I. Chafsey, et al., Protein cell surface display in Gram-positive bacteria: from single protein to macromolecular protein structure, FEMS Microbiol. Lett. 256 (2006) 1-15. https://doi.org/10.1111/j.1574-6968.2006.00122.x.

[9] R.A. Siciliano, R. Lippolis, M.F. Mazzeo, Proteomics for the investigation of surface-exposed proteins in probiotics, Front. Nutr. 6 (2019) 52. https://doi.org/10.3389/fnut.2019.00052.

[10] A.P.A. Hendrickx, R.J.L. Willems, M.J.M. Bonten, et al., LPxTG surface proteins of enterococci, Trends Microbiol. 17 (2009) 423-430. https://doi.org/10.1016/j.tim.2009.06.004.

[11] S. Lu, M. Ou, Q. Ye, et al., A novel strategy for designing the antioxidant and adhesive bifunctional protein using the *Lactobacillus* strain-derived LPxTG motif structure, Process Biochem. 127 (2023) 21-32. https://doi.org/10.1016/j.procbio.2023.01.019.

[12] I. von Ossowski, R. Satokari, J. Reunanen, et al., Functional characterization of a mucus-specific LPXTG surface adhesin from probiotic *Lactobacillus rhamnosus* GG, Appl. Environ. Microbiol. 77 (2011) 4465-4472. https://doi.org/10.1128/aem.02497-10.

[13] Z. Niu, M. Zou, T. Bei, et al., Effect of fructooligosaccharides on the colonization of *Lactobacillus rhamnosus* AS 1.2466T in the gut of mice, Food Sci. Hum. Wellness 12 (2023) 607-613. https://doi.org/10.1016/j.fshw.2022.07.063.

[14] K. Nishiyama, M. Sugiyama, T. Mukai, Adhesion properties of lactic acid bacteria on intestinal mucin, Microorganisms 4 (2016) 34. https://doi.org/10.3390/microorganisms4030034.

[15] K. Crampon, A. Giorkallos, M. Deldossi, et al., Machine-learning methods for ligand-protein molecular docking, Drug Discov. Today 27 (2022) 151-164. https://doi.org/10.1016/j.drudis.2021.09.007.

[16] J. Fan, A. Fu, L. Zhang, Progress in molecular docking, Quant. Biol. 7 (2019) 83-89. https://doi.org/10.1007/s40484-019-0172-y.

[17] M. Rosell, J. Fernández-Recio, Docking-based identification of small-molecule binding sites at protein-protein interfaces, Comput. Struct. Biotechnol. J. 18 (2020) 3750-3761. https://doi.org/10.1016/j.csbj.2020.11.029.

[18] A. Ioannou, C. Varotsis, Probing hemoglobin glyco-products by fluorescence spectroscopy, RSC Adv. 9 (2019) 37614-37619. https://doi.org/10.1039/c9ra05243g.

[19] D.M. Rogers, S.B. Jasim, N.T. Dyer, et al., Electronic circular dichroism spectroscopy of proteins, Chem. 5 (2019) 2751-2774. https://doi.org/10.1016/j.chempr.2019.07.008.

[20] J. Chamani, Comparison of the conformational stability of the non-native α-helical intermediate of thiol-modified β-lactoglobulin upon interaction with sodium *n*-alkyl sulfates at two different pH, J. Colloid Interface Sci. 299 (2006) 636-646. https://doi.org/10.1016/j.jcis.2006.02.049.

[21] A. Sharifi-Rad, J. Mehrzad, M. Darroudi, et al., Oil-in-water nanoemulsions comprising Berberine in olive oil: biological activities, binding mechanisms to human serum albumin or holo-transferrin and QMMD simulations, J. Biomol. Struct. Dyn. 39 (2021) 1029-1043. https://doi.org/10.1080/07391102.2020.1724568.

[22] H. Maheri, F. Hashemzadeh, N. Shakibapour, et al., Glucokinase activity enhancement by cellulose nanocrystals isolated from jujube seed: a novel perspective for type II diabetes mellitus treatment (*in vitro*), J. Mol. Struct. 1269 (2022) 133803. https://doi.org/10.1016/j.molstruc.2022.133803.

[23] Z. Malek-Esfandiari, A. Rezvani-Noghani, T. Sohrabi, et al., Molecular dynamics and multi-spectroscopic of the interaction behavior between bladder cancer cells and calf thymus DNA with rebeccamycin: apoptosis through the down regulation of PI3K/AKT signaling pathway, J. Fluoresc. 33 (2023) 1537-1557. https://doi.org/10.1007/s10895-023-03169-4.

[24] M. Kabiri, Z. Amiri-Tehranizadeh, A. Baratian, et al., Use of spectroscopic, zeta potential and molecular dynamic techniques to study the interaction between human holo-transferrin and two antagonist drugs: comparison of binary and ternary systems, Molecules 17 (2012) 3114-3147. https://doi.org/10.3390/molecules17033114.

[25] P. Baaske, C.J. Wienken, P. Reineck, et al., Optical thermophoresis for quantifying the buffer dependence of aptamer binding, Angew. Chem. Int. Ed. 49 (2010) 2238-2241. https://doi.org/10.1002/anie.200903998.

[26] N.N. Condurache, I. Aprodu, L. Grigore-Gurgu, et al., Fluorescence spectroscopy and molecular modeling of anthocyanins binding to bovine lactoferrin peptides, Food Chem. 318 (2020) 126508. https://doi.org/10.1016/j.foodchem.2020.126508

[27] J.F. Li, C.Y. Li, R.F. Aroca, Plasmon-enhanced fluorescence spectroscopy, Chem. Soc. Rev. 46 (2017) 3962-3979. https://doi.org/ 10.1039/c7cs00169j.

[28] A.J. Miles, R.W. Janes, B.A. Wallace, Tools and methods for circular dichroism spectroscopy of proteins: a tutorial review, Chem. Soc. Rev. 50 (2021) 8400-8413. https://doi.org/10.1039/d0cs00558d.

[29] D.P. Ronglu, Zhen W, Yuxing G, et al., Structure and immunomodulatory activity of a recombinant mucus-binding protein of *Lactobacillus acidophilus*, Future Microbiol. 13 (2018) 222. https://doi.org/10.2217/fmb-2018-0222.

[30] T. Gaillard, Evaluation of AutoDock and AutoDock vina on the CASF-2013 benchmark, J. Chem. Inf. Model. 58 (2018) 1697-1706. https://doi.org/10.1021/acs.jcim.8b00312.

[31] J.W. Arnold, J. Roach, S. Fabela, et al., The pleiotropic effects of prebiotic galacto-oligosaccharides on the aging gut, Microbiome 9 (2021) 31. https://doi.org/10.1186/s40168-020-00980-0.

[32] K. Sheng, S. He, M. Sun, et al., Synbiotic supplementation containing *Bifidobacterium infantis* and xylooligosaccharides alleviates dextran sulfate sodium-induced ulcerative colitis, Food Funct. 11 (2020) 3964-3974. https://doi.org/10.1039/d0fo00518e.

[33] R. Yazbeck, R.J. Lindsay, M.S. Geier, et al., Prebiotics fructo-, galacto-, and mannan-oligosaccharide do not protect against 5-fluorouracil-induced intestinal mucositis in rats, J. Nutr. 149 (2019) 2164-2173. https://doi.org/10.1093/jn/nxz192.

[34] D.N. Bronner, F. Faber, E.E. Olsan, et al., Genetic ablation of butyrate utilization attenuates gastrointestinal salmonella disease, Cell Host Microbe 23 (2018) 266-273. https://doi.org/10.1016/j.chom.2018.01.004.

[35] K. Obara, A. Kawaguchi, R. Inaba, et al., Docosahexaenoic acid and eicosapentaenoic acid inhibit the contractile responses of the guinea pig lower gastrointestinal tract, Biol. Pharm. Bull. 44 (2021) 1129-1139. https://doi.org/10.1248/bpb.b21-00362.

[36] M. Kristensen, S.R. Juul, K.V. Sorensen, et al., Supplementation with dairy calcium and/or flaxseed fibers in conjunction with orlistat augments fecal fat excretion without altering ratings of gastrointestinal comfort, Nutr. Metab. (Lond.) 14 (2017) 13. https://doi.org/10.1186/s12986-017-0164-8.

[37] G. Faa, V.M. Nurchi, A. Ravarino, et al., Zinc in gastrointestinal and liver disease, Coord. Chem. Rev. 252 (2008) 1257-1269. https://doi.org/10.1016/j.ccr.2007.09.024.

[38] G.C. Guimarães, H.R.M. Piva, G.C. Araújo, et al., Binding investigation between M2-1protein from hRSV and acetylated quercetin derivatives: ^{1}H NMR, fluorescence spectroscopy, and molecular docking, Int. J. Biol. Macromol. 111 (2018) 33-38. https://doi.org/10.1016/j.ijbiomac.2017.12.141.

[39] J. Liu, L. Jiang, Y. Zhang, et al., Binding behaviors and structural characteristics of ternary complexes of β-lactoglobulin, curcumin, and fatty acids, RSC Adv. 7 (2017) 45960-45967. https://doi.org/10.1039/c7ra09012a.

[40] L. Cai, X. Qin, Z. Xu, et al., Comparison of cytotoxicity evaluation of anticancer drugs between real-time cell analysis and CCK-8 method, ACS Omega 4 (2019) 12036-12042. https://doi.org/10.1021/acsomega.9b01142.

[41] B. Carbonetto, T. Nidelet, S. Guezenec, et al., Interactions between *Kazachstania humilis* yeast species and lactic acid bacteria in sourdough, Microorganisms 8 (2020) 240. https://doi.org/10.3390/microorganisms8020240.

[42] S. Sieuwerts, P.A. Bron, E.J. Smid, Mutually stimulating interactions between lactic acid bacteria and *Saccharomyces cerevisiae* in sourdough fermentation, LWT 90 (2018) 201-206. https://doi.org/10.1016/j.lwt.2017.12.022.

[43] Y. Wang, J. Wu, M. Lyu, et al., Metabolism characteristics of lactic acid bacteria and the expanding applications in food industry, Front. Bioeng. Biotechnol. 9 (2021) 612285. https://doi.org/10.3389/fbioe.2021.612285.

[44] Y. Xiao, J. Zhao, H. Zhang, et al., Mining *Lactobacillus* and *Bifidobacterium* for organisms with long-term gut colonization potential, Clin. Nutr. 39 (2020) 1315-1323. https://doi.org/10.1016/j.clnu.2019.05.014.

[45] J.R. Davies, G. Svensäter, M.C. Herzberg, Identification of novel LPXTG-linked surface proteins from *Streptococcus gordonii*, Microbiology 155 (2009) 1977-1988. https://doi.org/10.1099/mic.0.027854-0.

[46] Z. Zhang, J. Lyu, L. Pan, et al., Roles and applications of probiotic *Lactobacillus* strains, Appl. Microbiol. Biotechnol. 102 (2018) 8135-8143. https://doi.org/10.1007/s00253-018-9217-9.

[47] N. Singh, N. Bhalla, Moonlighting proteins, Annu. Rev. Genet. 54 (2020) 265-285. https://doi.org/10.1146/annurev-genet-030620-102906.

[48] G.M. da Costa, J.V. de Carvalho Silva, J.D. Mingotti, et al., Effect of ascorbic acid or oligofructose supplementation on *L. paracasei* viability, physicochemical characteristics and acceptance of probiotic orange juice, LWT 75 (2017) 195-201. https://doi.org/10.1016/j.lwt.2016.08.051.

[49] H.F. Jenkinson, Anchorless adhesins and invasins of Gram-positive bacteria: a new class of virulence factors, Trends Microbiol. 10 (2002) 205-208. https://doi.org/10.1016/s0966-842x(02)02351-x.

[50] Y. Terao, S. Kawabata, E. Kunitomo, et al., Fba, a novel fibronectin-binding protein from *Streptococcus pyogenes*, promotes bacterial entry into epithelial cells, and the *fba* gene is positively transcribed under the Mga regulator, Mol. Microbiol. 42 (2008) 75-86. https://doi.org/10.1046/j.1365-2958.2001.02579.x.

[51] H. Xu, L. Wu, D. Pan, et al., Adhesion characteristics and dual transcriptomic and proteomic analysis of *Lactobacillus reuteri* SH23 upon gastrointestinal fluid stress, J. Proteome Res. 20 (2021) 2447-2457. https://doi.org/10.1021/acs.jproteome.0c00933.

[52] K. Matsuo, Y. Sakurada, R. Yonehara, et al., Secondary-structure analysis of denatured proteins by vacuum-ultraviolet circular dichroism spectroscopy, Biophys. J. 92 (2007) 4088-4096. https://doi.org/10.1529/biophysj.106.103515.

[53] F. Mohammadi, A.K. Bordbar, A. Divsalar, et al., Interaction of curcumin and diacetylcurcumin with the lipocalin member β-lactoglobulin, Protein J. 28 (2009) 117-123. https://doi.org/10.1007/s10930-009-9171-6.

[54] M. Mejáre, L. Bülow, Metal-binding proteins and peptides in bioremediation and phytoremediation of heavy metals, Trends Biotechnol. 19 (2001) 67-73. https://doi.org/10.1016/s0167-7799(00)01534-1.

[55] R.P. Fagan, N.F. Fairweather, Biogenesis and functions of bacterial S-layers, Nat. Rev. Microbiol. 12 (2014) 211-222. https://doi.org/10.1038/nrmicro3213.

[56] N.S. de Alcântara-Contessoto, Í.P. Caruso, D.P. Bezerra, et al., An investigation into the interaction between piplartine (piperlongumine) and human serum albumin, Spectrochim. Acta A Mol. Biomol. Spectrosc. 220 (2019) 76. https://doi.org/10.1016/j.saa.2019.04.076.

[57] H.Y. Hsueh, P.Y. Yueh, B. Yu, et al., Expression of *Lactobacillus reuteri* Pg4 collagen-binding protein gene in *Lactobacillus casei* ATCC 393 increases its adhesion ability to Caco-2 cells, J. Agric. Food Chem. 58 (2010) 12182-12191. https://doi.org/10.1021/jf1035756.

[58] T. Wang, H. Sun, J. Chen, et al., Anti-Adhesion effects of *Lactobacillus* strains on Caco-2 cells against *Escherichia coli* and their application in ameliorating the symptoms of dextran sulfate sodium-induced colitis in mice, Probiotics Antimicrob. Proteins 13 (2021) 1632-1643. https://doi.org/10.1007/s12602-021-09774-8.

[59] E.F. Garcia, W.A. Luciano, D.E. Xavier, et al., Identification of lactic acid bacteria in fruit pulp processing byproducts and potential probiotic properties of selected *Lactobacillus* strains, Front. Microbiol. 7 (2016) 1371. https://doi.org/10.3389/fmicb.2016.01371.

[60] K. Ramiah, C.A. van Reenen, L.M.T. Dicks, Surface-bound proteins of *Lactobacillus plantarum* 423 that contribute to adhesion of Caco-2 cells and their role in competitive exclusion and displacement of *Clostridium sporogenes* and *Enterococcus faecalis*, Res. Microbiol. 159 (2008) 470-475. https://doi.org/10.1016/j.resmic.2008.06.002.